Article

Not peer-reviewed version

Dosimetric Assessment of Multi-Frequency Smartwatch Electromagnetic Exposure on Children's Sensitive Organs

Mingfei Luo , Wenqi Hou , Wenying Zhou *

Posted Date: 13 March 2026

doi: 10.20944/preprints202603.1048.v1

Keywords: dosimetric assessment; electromagnetic exposure; multi-frequency smartwatches; children's sensitive organs; radiation dose

 doi:10.20944/preprints202603.1048.v1

Article

Dosimetric Assessment of Multi-Frequency Smartwatch Electromagnetic Exposure on Children's Sensitive Organs

Mingfei Luo [1], Wenqi Hou [1] and Wenying Zhou [1,2,*]

[1] Key Laboratory of Opto-Electronic Technology and Intelligent Control of Ministry of Education, Lanzhou Jiaotong University, Lanzhou, China

[2] School of Information Science and Engineering, Lanzhou University, Lanzhou, China

* Correspondence: zhouwy29@126.com

Abstract

To assess the electromagnetic effect on the children's sensitive organs when they using the smartwatches, this study analyzes the electromagnetic dose absorbed by the children, especially calculate the combind electromagnetic exposure, We propose a multi-frequency smartwatch antenna (GPS L1, LTE FDD band1, 2.4G Wi-Fi/Bluetooth) and construct a 6-year-old human model including ten tissues from three sensitive organs (brain, eyes, heart). The Specific Absorption Rate (SAR) distributions are simulated under speaking and listening postures at different frequencies using CST Studio Suite. Furthermore, the SAR distributions under multi-frequency combined electromagnetic exposure are evaluated to investigate the superposition effects of electromagnetic fields. The results show that, when the child uses the smartwatch for 4G communication in the listening posture, the maximum local SAR reaches 1.683 W/kg, which is nearly half of the ICNIRP exposure limit. Electromagnetic radiation in the child's brain is mainly concentrated on the surface of the cerebrum and cerebellum, while the radiation in the eyes is mainly distributed in the outer and anterior tissues. Under combined electromagnetic exposure, the SAR values of tissues increase by 1.17 to 3.53 times compared with single-frequency conditions but remain within safety limits. Considering the long-term use of smartwatches, the potential health risks to developing children still deserve attention.

Keywords: dosimetric assessment; electromagnetic exposure; multi-frequency smartwatches; children's sensitive organs; radiation dose

1. Introduction

In recent years, children's smartwatches have rapidly gained popularity among children's groups by virtue of their convenience and multi-functionality. According to statistics, nearly one-third of China's 170 million children between the ages of 5 and 12 have smartwatches, moreover, the market penetration rate of children's smartwatches in cities is more than half[1]. Children's smartwatches not only meet the needs of modern communication, but also integrate a variety of functions, including positioning, learning, and entertainment, which greatly extend the usage time of the devices. In 2000, the Independent Expert Group on Mobile Phones (IEGMP) pointed out the potential risks of children using electronic devices[2]. Children's nervous systems are still in the developmental stage. Compared to adults, children have smaller heads, thinner skulls, and higher moisture content in their body tissues, which makes them more sensitive to radio frequency (RF) radiation. In addition, the trend of younger children using smartwatches leads to higher health risks of electromagnetic radiation. In 2013, the International Agency for Research on Cancer (IARC/WHO) classified RF electromagnetic field as Group 2B carcinogens[3], and the cumulative effect of radiation further aggravates the public's concern about the effects of RF EMF on children's health.

 doi:10.20944/preprints202603.1048.v1

Epidemiological and experimental studies have shown that long-term or excessive exposure to radio-frequency (RF) radiation is significantly associated with children's health, such as impaired multitasking ability[4] and decreased sleep quality[5]. Studies have found that RF electromagnetic radiation may cause damage to the cerebrum and cerebellum[6,7] and affect the developmental stages of the nervous system, thereby potentially influencing subsequent cognitive functions[8]. Within the resonance frequency range, the deep thalamus tissue may absorb even more electromagnetic energy than the external brain tissues[9]. In addition, because the eyeball lacks the protection of skin, prolonged direct exposure to electromagnetic fields may damage important ocular tissues such as the lens[10], cornea[11], and retina[12]. Experimental studies using near-field mobile phone electromagnetic waves have also indicated that ocular tissues may exhibit biological responses to RF exposure[13]. Furthermore, RF electromagnetic radiation may affect the cardiovascular system[14] and induce myocardial injury[15], thereby impairing the heart's blood supply function. These studies suggest that the brain, eyes, and heart are particularly sensitive to electromagnetic radiation due to their critical physiological functions and unique anatomical locations, especially in the more vulnerable pediatric population[16].With the rapid development of wearable devices, children's smartwatches have been widely used for communication, positioning, and entertainment. When children use these devices, the RF electromagnetic radiation generated by the antennas may expose the aforementioned sensitive tissues to prolonged electromagnetic fields. Although numerous studies have evaluated electromagnetic exposure from mobile devices using computational electromagnetics, most investigations focus on traditional devices such as mobile phones, tablets[17], and laptops[18]. Research on electromagnetic exposure from smartwatch antennas remains relatively limited, and existing studies mainly examine the effects of electromagnetic exposure on partial human tissues[19], typically using simplified adult hand models. Considering that children have smaller head structures and higher body water content, the radiation dose they absorb under the same conditions may be significantly higher than that of adults, potentially exceeding the adult dose by up to an order of magnitude[20]. Therefore, it is necessary to systematically investigate the RF electromagnetic exposure of sensitive tissues when children use smartwatches.

To accurately evaluate the electromagnetic radiation dose absorbed by children's sensitive tissues, this study constructs a multi-frequency smartwatch antenna and a child model containing three sensitive organs: the brain, eyes, and heart. The brain is further subdivided into the cerebrum, cerebellum, and thalamus, while the eye is divided into five tissues including the cornea, anterior chamber, lens, sclera, and vitreous humor. Based on the finite integral technique (FIT) implemented in CST Studio Suite, the SAR distributions in these tissues are simulated under two typical smartwatch usage postures, namely speaking and listening, at different operating frequencies. Furthermore, considering that modern smartwatches often operate with multiple wireless communication modules simultaneously, the SAR distributions under combined multi-frequency electromagnetic exposure are also evaluated to investigate the superposition effect of electromagnetic fields on human tissues. The obtained results provide theoretical support for evaluating electromagnetic exposure safety and for optimizing the antenna design and electromagnetic protection strategies for children's smartwatches.

2. Electromagnetic Exposure Model

2.1. Design of a Multi-Frequency Smartwatch

The children's smartwatch studied in this article is for children aged between 3 and 14 years old[21]. According to the actual use requirements, a multi-frequency children's smartwatch integrating positioning, calling, Wi-Fi and Bluetooth functions is constructed. Through optimizing the radiation performance of the antennas[22] to meet the communication needs of children nowadays, remove the resistive elements to simplify the antenna structure, and adjust the operating frequency band from GSM to LTE FDD. The optimized smartwatch and its geometric parameters are shown in Figure 1. The dual-band microstrip antenna at the top of the watch is used for calls which

 doi:10.20944/preprints202603.1048.v1

covers the LTE FDD band1 (1920-1980 MHz, 2110-2170 MHz), while the dual-band microstrip antenna at the bottom covers the GPS L1 frequency (1575.42 MHz) as well as the 2.4G Wi-Fi and Bluetooth band (2400 MHz-2483.5 MHz).

The microstrip antennas in Figure 1 are all printed on a 0.4 mm thick FR-4 substrate with dielectric constant of 4.4 and loss tangent of 0.02. The antennas on both the top and bottom sides have dimensions of 35 mm × 5 mm × 2 mm, and a metal ground plate with dimensions of 34.2 mm × 44.2 mm is connected in the middle.

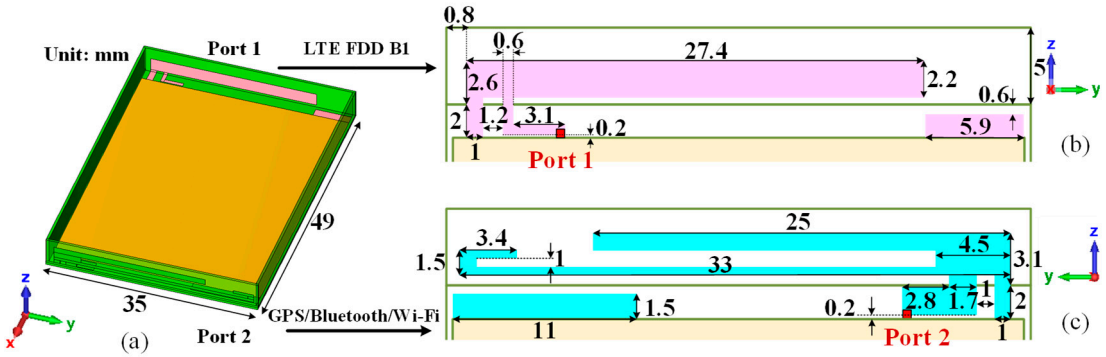

Figure 1. Smartwatch model. (a)The whole antenna. (b)The top antenna. (c)The bottom antenna.

The simulation results of the radiation performance of the proposed antennas are shown in Figure 2. S_{11} represents the reflection coefficient of the top antenna (Port 1), S_{22} represents the reflection coefficient of the bottom antenna (Port 2), and S_{21} indicates the isolation between the two antennas.

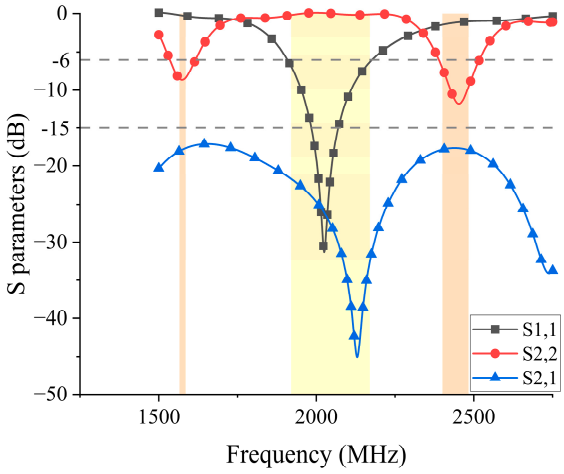

Figure 2. S-parameter of the smartwatch antenna.

Figure 2 shows that the top antenna has an operating bandwidth of 265 MHz (1909 MHz-2174 MHz), which covers the LTE FDD band1 (1920-1980 MHz, 2110-2170 MHz), and the bottom antenna has operating bandwidths of 76 MHz (1538 MHz-1614 MHz) and 127 MHz (2389 MHz-2516 MHz) respectively, covering the GPS L1 frequency (1575.42 MHz) and 2.4G Wi-Fi and Bluetooth bands (2400 MHz-2483.5 MHz).

Figure 3 shows that, when the antenna operates at 1575 MHz, 2045 MHz, and 2450 MHz, the maximum gain of the antenna is 2.24 dBi, 2.69 dBi and 3.10 dBi.

 doi:10.20944/preprints202603.1048.v1

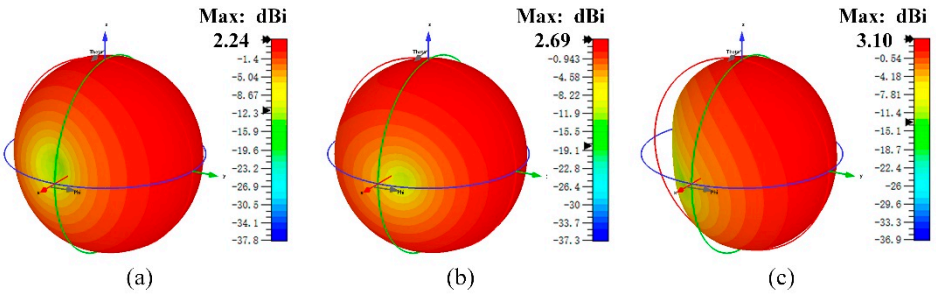

Figure 3. Antenna gain (3D) at (a) 1575 MHz, (b) 2045 MHz, (c) 2450 MHz.

The above results show the proposed children's smartwatch meets the required radiation performance to enable the functions of calling, positioning and internet access.

2.2. Construction of the Child Model

This study refers to the Chinese human body size standard for underage males[23] to construct a 6-year-old boy's human body model[24] with a height of 119.3 cm. Based on epidemiologically suggested risks and sensitivities to organ development in children, we construct three sensitive organs, which are the brain, the eyes, and the heart, as shown in Figure 4. The brain organ is refined into the cerebellum, thalamus, and other parts. Based on the average ocular axis length of 6-year-old children in China[25], we construct the eye model with an axial length of 22.5 mm. The eye model contains 5 tissues, including cornea, anterior chamber, lens, sclera and vitreous humor. Figure 4(a) and 4(b) show the speaking posture and the listening posture, respectively. Considering the real usage conditions and product dimensions, in two postures, the distance between the antenna model and the child's arm remains approximately 3 mm, and the separation distance between the antenna model and the head is about 30 mm.

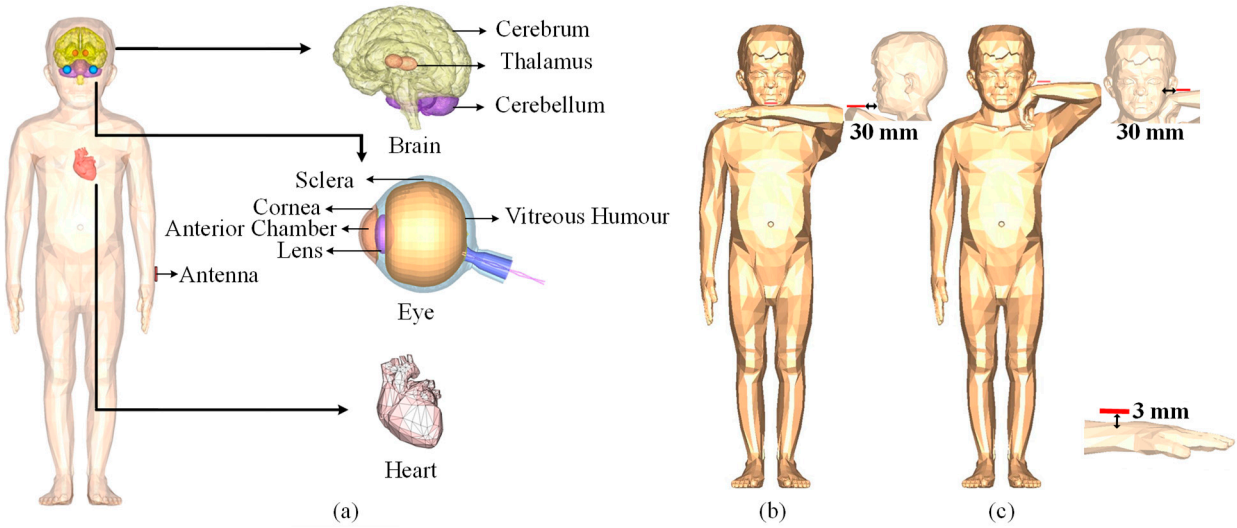

Figure 4. Child models: (a) Distribution of human organs and tissues; (b)Speaking; (c) Listening.

To evaluate the radiation impact of the smartwatch antenna on children in different postures, numerical simulations of the child model in the speaking and listening postures were conducted in CST Studio Suite, as shown in the Figure 5.The computational domain was enclosed by a bounding box with open (add space) boundary conditions applied to all six sides to simulate free-space radiation. The child model in the speaking posture was discretized into 79.31 million meshcells, and the model in the listening posture was discretized into 63.36 million meshcells.The input power of the watch antenna in the speaking and listening postures is 0.05 W.

 doi:10.20944/preprints202603.1048.v1

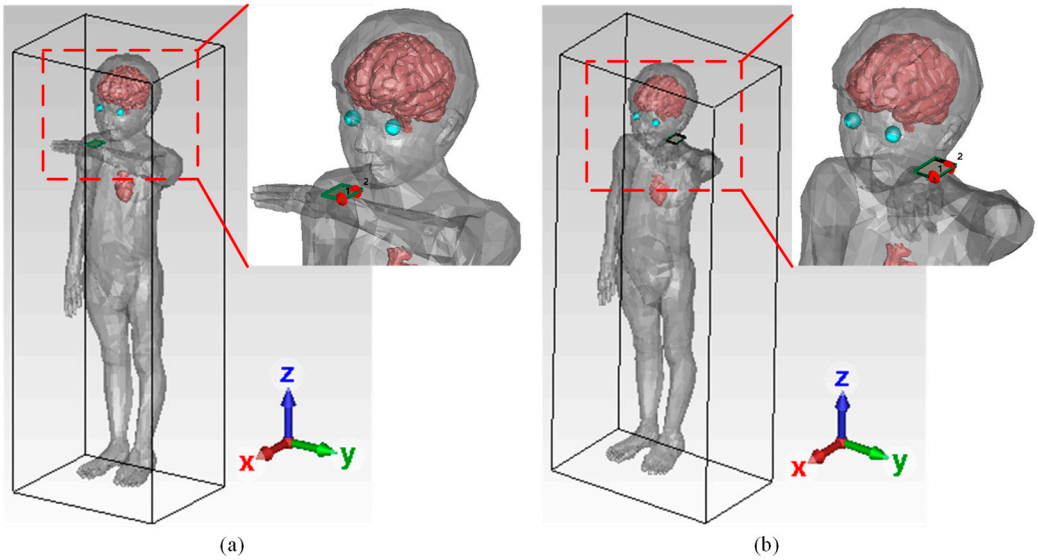

(a) (b)

Figure 5. Numerical simulation model: (a) Speaking; (b) Listening.

The relative permittivity ε and conductivity σ of different tissues of the human body at various frequencies are calculated using the 4-Cole-Cole model[26], as illustrated in Table 1.

Table 1. Dielectric properties of tissues at different frequencies.

Human Tissues	2045 MHz		2450 MHz	
	ε	σ (S/m)	ε	σ (S/m)
Muscle	53.233	1.480	52.729	1.739
Gray Matter of Brain	49.609	1.539	48.911	1.808
White Matter of Brain	36.672	1.022	36.167	1.215
Cerebellum	45.574	1.850	44.804	2.101
Cornea	52.308	2.013	51.615	2.295
Body Fluid	68.448	2.185	68.208	2.478
Lens	45.075	1.272	44.625	1.504
Vitreous Humor	68.448	2.185	68.208	2.478
Sclera	53.205	1.753	52.628	2.033
Heart	55.708	1.944	54.814	2.256

3. Radiation Impacts of Smartwatches on Child with Different Postures

Since it is difficult to directly measure the electromagnetic dose in the human body, numerical calculations are commonly used to evaluate the safety of electromagnetic exposure[27]. In the guidelines developed by the ICNIRP, SAR is used to measure the electromagnetic exposure energy absorbed per unit mass of human tissue per unit time[28], which can be expressed as:

$$\mathrm{SAR} = \frac{\sigma|\mathrm{E}|^2}{\rho} \quad (1)$$

where E is the electric field strength (V/m), σ is the conductivity of the biological tissue (S/m), and ρ is the mass density (kg/m3).

3.1. Construction of the Child Model

 doi:10.20944/preprints202603.1048.v1

Considering the actual use of the smartwatch, it is worn on the left wrist of the child model. The values of SAR absorbed by the child body in the two postures of speaking and listening are shown in Table 2 when the watch antenna operates at 4G communication frequency point 2045 MHz, and Wi-Fi frequency point 2450 MHz, respectively.

Table 2. Peak values of local SAR10g (W/kg) values at different frequencies for different tissues of a child's body in two different postures.

Postures	Frequencies	Local Brain	Local Eyes	Local Heart	Local Limb
Speaking	2045 MHz	1.804×10^{-3}	2.676×10^{-3}	3.389×10^{-5}	1.415
	2450 MHz	4.091×10^{-3}	5.727×10^{-3}	7.513×10^{-5}	0.722
Listening	2045 MHz	3.933×10^{-3}	4.539×10^{-3}	3.272×10^{-5}	1.683
	2450 MHz	7.701×10^{-3}	7.316×10^{-3}	2.376×10^{-5}	0.666
ICNIRP public restriction value	100 kHz to 6 GHz	Local Head/Torso: 2.000			4.000

Comparing the maximum SAR values absorbed by each tissue at different postures and different operating frequencies of the smartwatch in Table 2, the conclusions are as follows:

(1) In two postures, the maximum local SAR in the child is observed in the limb, specifically the left wrist where the smartwatch is worn. When the child wears the smartwatch in the listening posture at a frequency of 2045 MHz, the limb local SAR reaches its maximum value of 1.683 W/kg.

(2) Comparison of the peak local SAR value absorbed by each tissue of the child in different postures is concluded as follows: a). In the speaking posture, the antenna of the smartwatch operates at the 2450 MHz frequency is positioned backward and close to the human face, therefore the radiation dose absorbed by the eye is the most, which is 5.727×10^{-3} W/kg. b). In the listening posture, the brain absorbs the most radiation dose, with a peak SAR value of 7.701×10^{-3} W/kg; the heart absorbs the lowest radiation dose, with a SAR value of 2.376×10-5 W/kg.

In order to further discuss the electromagnetic exposure to different tissues in the three sensitive organs of the child with different postures, the distribution of radiation dose absorbed by specific tissues in the child's body was analyzed at different frequencies.

3.2. Distribution of Radiation Dose in Child's Body with Speaking Posture

The electromagnetic exposure of various tissues in the child's body with the speaking posture when smartwatch operates at 2045 MHz and 2450 MHz, respectively, are shown in Figure 6.

 doi:10.20944/preprints202603.1048.v1

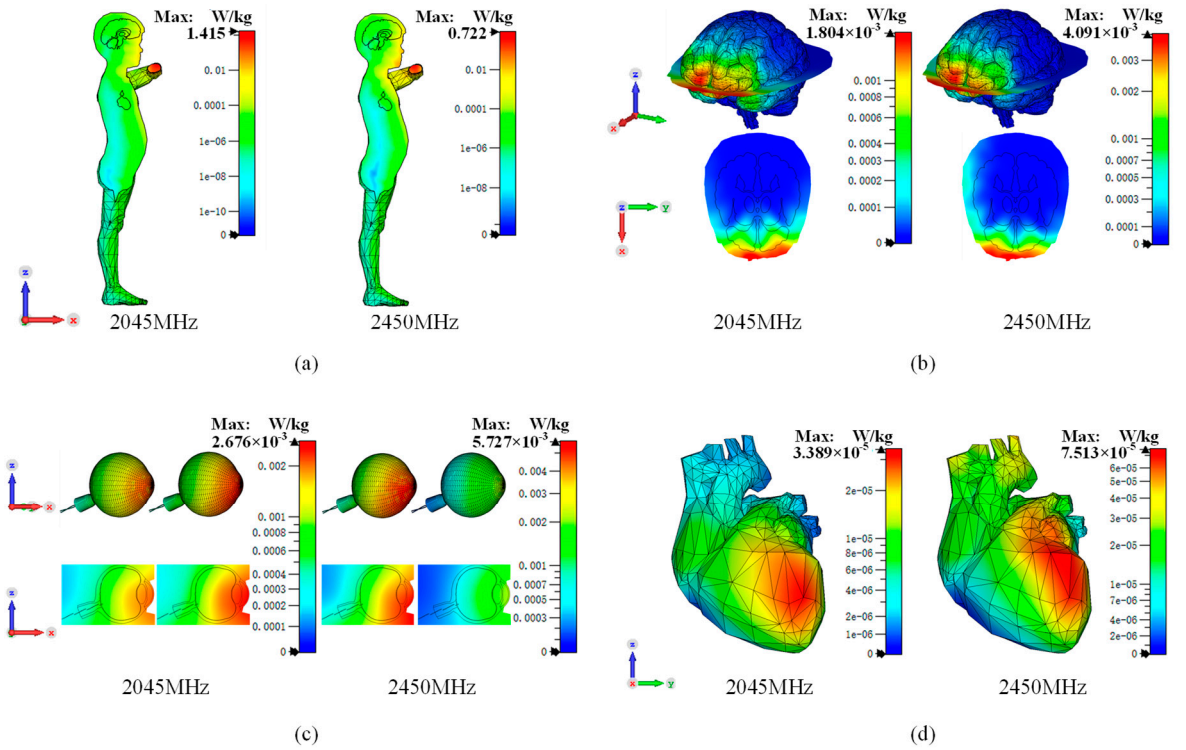

Figure 6. SAR distribution of various tissues of the child model with speaking posture: (a) Whole body; (b) Brain; (c) Eyes; (d) Heart.

Figure 6 shows that the SAR is mainly concentrated in the anterior part of the upper body and decreases with the increase of the skin depth, and the absorbed radiation of the left arm and face is significantly more than that of the other parts. The SAR distribution in various tissues is concluded as follows:

The absorption of electromagnetic radiation in brain tissue is primarily concentrated in the cerebrum, followed by the cerebellum, while the thalamus absorbs the lowest radiation dose. At different operating frequencies, the SAR distribution in the brain is mainly concentrated in the right frontal lobe of the cerebrum, with a maximum SAR value of 4.091×10^{-3} W/kg. In contrast, the SAR values in deep brain tissues are significantly lower, generally not exceeding 1% of the maximum SAR value in brain tissue, indicating that deep brain regions are less affected by electromagnetic radiation.

The absorbed electromagnetic radiation dose in the eyes is positively correlated with the operating frequency of the antenna. The distribution of radiation dose in both eyes exhibits an anterior-to-posterior decreasing trend, with the maximum values occurring at the cornea. When the antenna operates at 2045 MHz, the maximum SAR value in the eye is located in the cornea of the left eye, with a value of 2.676×10^{-3} W/kg; when the antenna operates at 2450 MHz, the maximum SAR value in the eye is located in the cornea of the right eye, with a value of 5.727×10^{-3} W/kg.

(3) Electromagnetic radiation penetrates deeper in the heart. The maximum SAR values are observed in the anterior aspect of the left ventricle at all operating frequencies, decreasing backward. When the smartwatch antenna operates at 2450 MHz, the maximum SAR value in the heart reaches 7.513×10^{-5} W/kg, which is approximately twice the maximum SAR value observed at 2045 MHz.

3.3. Distribution of Radiation Dose in Child's Body with Listening Posture

The electromagnetic exposure of various tissues in the child's body with the listening posture when smartwatch operates at 2045 MHz and 2450 MHz, respectively, are shown in 7.

Figure 7 shows that the whole-body SAR is mainly distributed on the left arm and the left side of the head. The distribution of SAR in each tissue is concluded as follows:

 doi:10.20944/preprints202603.1048.v1

(1) The electromagnetic radiation absorbed by the brain is mainly distributed in the left hemisphere of the cerebrum. When the antenna operates at 2045 MHz, the maximum SAR value in the cerebrum appears in the frontal lobe, with an observed maximum SAR of 3.933×10^{-3} W/kg. When the antenna operates at 2450 MHz, the maximum SAR value in the cerebrum appears in the temporal lobe, with an observed maximum SAR of 7.701×10^{-3} W/kg. For the cerebellum and thalamus, the absorbed electromagnetic radiation is primarily concentrated in the left hemisphere, with both achieving their maximum SAR values at the operating frequency of 2450 MHz, which are 1.184×10^{-3} W/kg and 1.455×10^{-4} W/kg, respectively.

(2) In the listening posture, when the antenna operates at 2045 MHz and 2450 MHz, the electromagnetic radiation absorbed by the eyes is mainly concentrated in the left eye, and the electromagnetic radiation dose gradually decreases from left to right. The maximum SAR value is located within the left sclera, with values reaching 4.539×10^{-3} W/kg and 7.316×10^{-3} W/kg, respectively.

(3) Electromagnetic radiation penetrates deeper in the heart. The maximum SAR values are observed in the anterior aspect of the left ventricle at all operating frequencies, decreasing backward. When the antenna operates at 2045 MHz, the maximum SAR value of the heart is 3.272×10^{-5} W/kg, and when the antenna operates at 2450 MHz, the maximum SAR value of the heart is 2.376×10^{-5} W/kg.

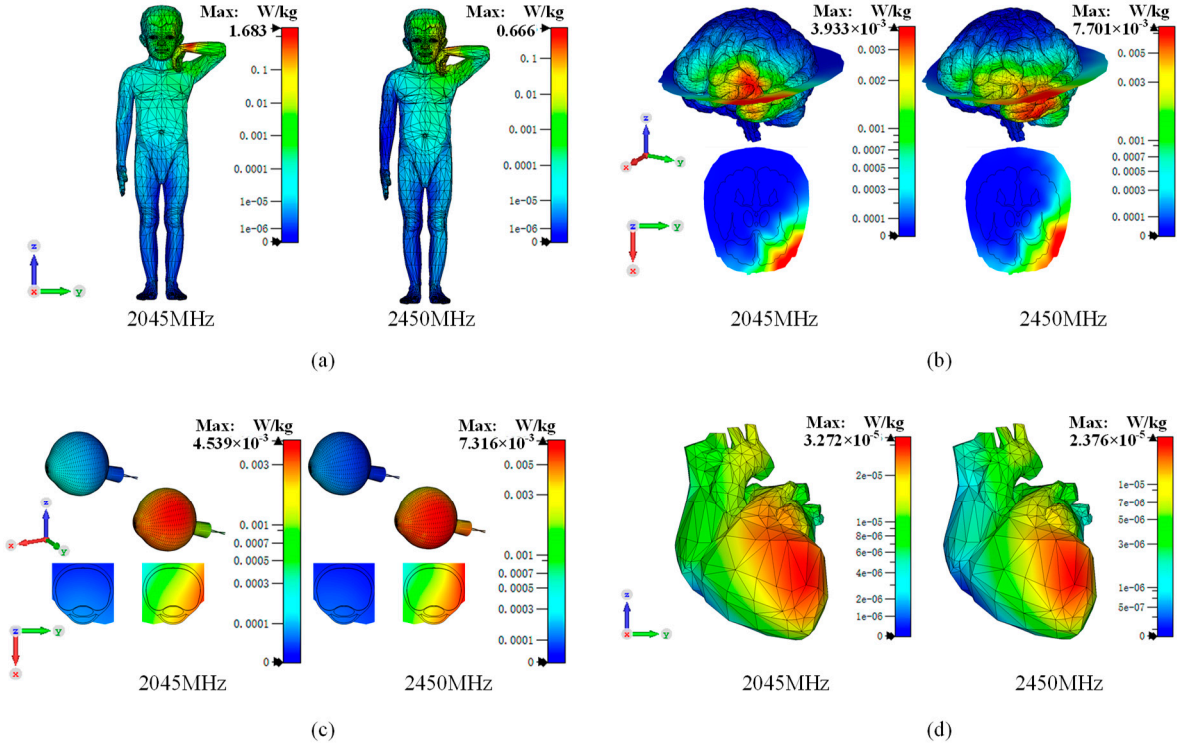

Figure 7. SAR distribution of various tissues of the child model with listening posture: (a) Whole body; (b) Brain; (c) Eyes; (d) Heart.

4. SAR Comparison Between Single and Combined EMF Exposure

In practical scenarios, children's smartwatches usually integrate multiple wireless communication functions, such as LTE, and Wi-Fi/Bluetooth. When these communication modules operate simultaneously, electromagnetic fields at different frequencies may coexist and superimpose around the human body, leading to combined electromagnetic exposure[29]. Therefore, it is necessary to compare the SAR distributions under single-frequency exposure and multi-frequency combined exposure[30]. The combined EMF of the SAR ($SAR_{combined}$) in different tissues exposed to two different frequencies is found according to the ICNIRP guideline, as shown in Equation 2.

$$SAR_{combined} = \frac{\int_v \sigma_{2045MHz} |E|^2_{2045MHz} dv + \int_v \sigma_{2450MHz} |E|^2_{2450MHz} dv}{\int_v \rho dv} \quad (2)$$

 doi:10.20944/preprints202603.1048.v1

Each permittivity and conductivity of each human tissue correspond to a single operating frequency of the mobile phone, where $V=\int_v dv$ is the volume of the integral.

Based on the above theoretical calculations, the CST Studio Suite software was used to simulate the peak SAR_{10g} values in different tissues of the human body model under a composite electromagnetic field environment at 2045 MHz and 2450 MHz. Figure 8 presents a comparative bar chart of the peak SAR_{10g} values under single-frequency and multi-frequency operating conditions.

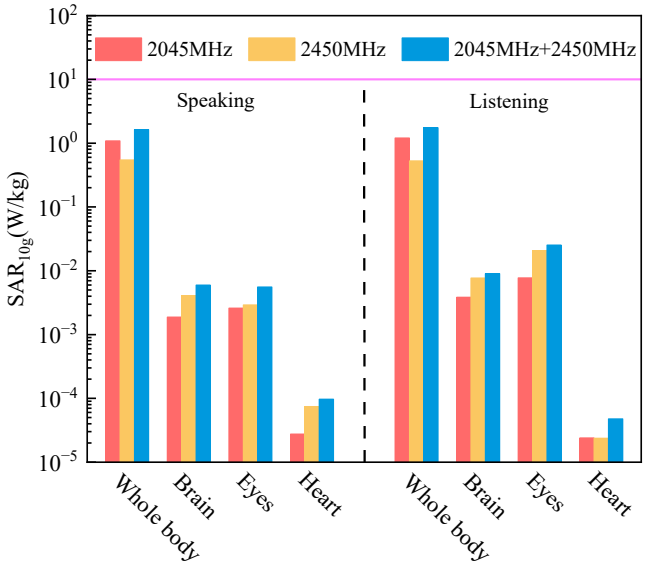

Figure 8. Comparison of peak SAR_{10g} in different tissues under single-frequency and combined exposure for different postures.

As shown in Figure 8, under both the listening and speaking postures, the peak SAR10g values of all tissues under the combined exposure of 2045 MHz and 2450 MHz are higher than those under single-frequency conditions. The increases range from approximately 1.17 to 3.53 times the corresponding peak SAR_{10g} values under single-frequency exposure. This indicates that the superposition of multi-frequency electromagnetic fields can increase the absorption of electromagnetic energy in human tissues.

In addition, the peak whole-body SAR_{10g} mainly occurs in the limb regions. According to the electromagnetic exposure safety limits shown in Table 2, the localized SAR limit for limbs (local limb) is 4 W/kg. Under the combined exposure condition, the peak SAR_{10g} values in the speaking and listening postures are 1.632 W/kg and 1.742 W/kg, respectively, both of which remain below the safety limit of 4 W/kg.For other tissues, such as the brain, eyes, and heart, the peak SAR_{10g} values are significantly lower than the localized SAR limit of 2 W/kg. Overall, although the multi-frequency superposition slightly increases the electromagnetic energy absorption in human tissues, all simulated SAR values remain within the safety limits under the conditions considered in this study.However, long-term exposure under multi-frequency operating conditions still deserves further investigation.

5. Conclusion

This study constructs a multi-frequency smartwatch and a child model that includes three sensitive organs: the brain, eyes, and heart. Based on the FIT method, the electromagnetic radiation distribution in various tissues of the child is simulated under speaking and listening postures when the smartwatch antenna operates at frequencies of 2045 MHz and 2450 MHz. The conclusions are as follows:

 doi:10.20944/preprints202603.1048.v1

(1) Comparison of the maximum SAR values absorbed in the child's body shows that across all postures and operating frequencies, the highest local SAR in the child is observed in the left wrist. The peak value of limb local SAR reaches 1.683 W/kg when the child uses the smartwatch for 4G communication in the listening posture. (2) Comparison of the electromagnetic radiation distribution under different postures shows that in the speaking posture, the eye absorbs the largest radiation dose, with a maximum SAR value of 5.727×10^{-3} W/kg. In the listening posture, the brain absorbs the largest radiation dose, with a maximum SAR value of 7.701×10^{-3} W/kg. This indicates that different postures determine the degree to which radiation is absorbed by different tissues in children. (3) Comparison of the electromagnetic radiation distribution across different tissues shows that electromagnetic radiation in the child's brain is mainly concentrated on the surface of the cerebrum and cerebellum. In the child's eyes, electromagnetic radiation is more concentrated in the cornea and sclera tissues. In the child's heart, SAR values exceed 40% of the maximum value in more than half of the heart tissue. (4) Under combined multi-frequency electromagnetic exposure, the peak SAR_{10g} values of all tissues increase compared with single-frequency exposure due to the superposition of electromagnetic fields. The increases range from approximately 1.17 to 3.53 times. The cumulative effects under long-term multi-frequency exposure conditions should be further investigated.

This study systematically assesses the electromagnetic exposure safety for various body tissues of children wearing smartwatches under different postures. Based on the results, it is recommended that children maintain an appropriate distance between the smartwatch and the head, particularly from the sensitive eyes, and limit the duration of using the speaking and listening functions. The findings of this study can assist in the antenna design of children's smartwatches and inform the development of electromagnetic protection standards. Reducing the impact of electromagnetic exposure on children by designing reflective surfaces on the back of children's smartwatches is our next work.

Author Contributions: Conceptualization, W.-Y.Z.; Methodology, W.-Y.Z.; Investigation, W.-Y.Z.; Writing—original draft, M.-F.L. and W.-Q.H.; Calculation, M.-F.L. and W.-Q.H.; Data analysis, M.-F.L. and W.-Q.H.; Funding acquisition, W.-Y.Z.; Supervision, W.-Y.Z. All authors have read and agreed to the published version of the manuscript.

Funding: This work was supported by the National Natural Science Foundation of China [grant numbers 62161017]; and the Zhiyuan Laboratory [grant number ZYL2024004].

Institutional Review Board Statement: Not applicable.

Informed Consent Statement: Not applicable.

Data Availability Statement: The original contributions presented in this study are included in the article. Further inquiries can be directed to the corresponding author.

Conflicts of Interest: The authors declare no competing interests.

References

1. Cao A (2023) China's Little Genius smartwatch for kids overtakes Apple Watch in home market thanks to features such as remote body temperature alerts. In: South China Morning Post. https://www.scmp.com/tech/tech-trends/article/3233502/chinas-little-genius-smartwatch-kids-overtakes-apple-watch-home-market-thanks-features-such-remote. Accessed 12 Oct 2024
2. Stewart W (2000) Mobile Phones and Health (The Stewart Report). Independent Expert Group On Mobile Phones, Chilton, UK
3. IARC Working Group on the Evaluation of Carcinogenic Risks to Humans (2013) Non-ionizing radiation, Part 2: Radiofrequency electromagnetic fields. IARC monographs on the evaluation of carcinogenic risks to humans, Lyon, France

 doi:10.20944/preprints202603.1048.v1

4. Shaer, R., Eldin, S. N., Gashri, C., & Horowitz-Kraus, T. (2024). Decreased frontal theta frequency during the presence of smartphone among children: An EEG study. Pediatric Research, 96(7), 1699–1706. https://doi.org/10.1038/s41390-024-03155-x
5. Cabré-Riera A, Torrent M, Donaire-Gonzalez D, et al (2019) Telecommunication devices use, screen time and sleep in adolescents. Environ Res 171:341–347. https://doi.org/10.1016/j.envres.2018.10.036
6. Hu, C., Zuo, H., & Li, Y. (2021). Effects of Radiofrequency Electromagnetic Radiation on Neurotransmitters in the Brain. Frontiers in Public Health, 9, 691880. https://doi.org/10.3389/fpubh.2021.691880
7. Singh KV, Prakash C, Nirala JP, et al (2023) Acute radiofrequency electromagnetic radiation exposure impairs neurogenesis and causes neuronal DNA damage in the young rat brain. NeuroToxicology 94:46–58. https://doi.org/10.1016/j.neuro.2022.11.001
8. Kim, J. H., Seok, J. Y., Kim, Y.-H., Kim, H. J., Lee, J.-K., & Kim, H. R. (2024). Exposure to Radiofrequency Induces Synaptic Dysfunction in Cortical Neurons Causing Learning and Memory Alteration in Early Postnatal Mice. International Journal of Molecular Sciences, 25(16), 8589. https://doi.org/10.3390/ijms25168589
9. Lee A-K, Choi H-D (2023) Dosimetric assessment in the brain for downlink EMF exposure in Korean mobile communication networks. Environ Res 234:116542. https://doi.org/10.1016/j.envres.2023.116542
10. Morishima, Y., Chida, K., Chiba, H., & Kumagai, K. (2024). Radiation dose to the eye of physicians during radio frequency catheter ablation: A small-scale study. Irish Journal of Medical Science, 193(6), 2745-2751. https://doi.org/10.1007/s11845-024-03802-6
11. Kojima, M., Tasaki, T., Kamijo, T., Hada, A., Suzuki, Y., Kik, A., Ikehata, M., & Sasaki, H. (2025). Investigation of the Ocular Response and Corneal Damage Threshold of Exposure to 28 GHz Quasi-millimeter Wave Exposure. Health Physics, 128(6), 487-496. https://doi.org/10.1097/HP.0000000000001951
12. Zhou X-R, Yuan H-P, Qu W, et al (2008) The Study of Retinal Ganglion Cell Apoptosis Induced by Different Intensities of Microwave Irradiation. Ophthalmologica 222:6–10. https://doi.org/10.1159/000109271
13. Bozorgmanesh, M. A., Honar, F., & Kowkabi, F. (2023). Investigating the Effect of Mobile Phone Electromagnetic Waves on the Human Eye. TechRxiv. https://doi.org/10.36227/techrxiv.22722562.v1
14. Michelant, L., & Selmaoui, B. (2025). Impact of Radiofrequency Electromagnetic Fields on Cardiac Activity at Rest: A Systematic Review of Healthy Human Studies. Bioelectromagnetics, 46(5), e70014. https://doi.org/10.1002/bem.70014
15. Li D, Xu X, Yin Y, et al (2023) Physiological and Psychological Stress of Microwave Radiation-Induced Cardiac Injury in Rats. Int J Mol Sci 24:6237. https://doi.org/10.3390/ijms24076237
16. Li, J. (2025). The association between smartphone use and myopia progression in children: A prospective cohort study. BMC Pediatrics, 25(1), 378. https://doi.org/10.1186/s12887-025-05715-4
17. Oliveira C, Mackowiak M, Correia LM (2015) Exposure assessment of smartphones and tablets. In: 2015 International Symposium on Wireless Communication Systems (ISWCS). IEEE, Brussels, pp 436–440
18. Soares NE, Bulla G, Fernandez-Rodriguez CE, De Salles AAA (2023) SAR Estimations in a Child Due to RF Exposures from Several Laptops in a Classroom Environment. In: 2023 IEEE MTT-S Latin America Microwave Conference (LAMC). IEEE, San José, Costa Rica, pp 58–60
19. Bhadrvathi Ghouse PS, Mane PR, Thankappan Sumangala S, et al (2023) A Compact Dual-Band Millimeter Wave Antenna for Smartwatch and IoT Applications with Link Budget Estimation. Sensors 24:103. https://doi.org/10.3390/s24010103
20. Fernández C, De Salles AA, Sears ME, et al (2018) Absorption of wireless radiation in the child versus adult brain and eye from cell phone conversation or virtual reality. Environ Res 167:694–699. https://doi.org/10.1016/j.envres.2018.05.013
21. State Administration for Market Regulation, Standardization Administration of the People's Republic of China (2022) Children's watches
22. Huang H-S, Su H-L, Chen S-L (2017) Multiband antennas for GPS/GSM1800/Bluetooth/Wi-Fi smart watch applications. In: 2017 IEEE International Conference on Computational Electromagnetics (ICCEM). IEEE, Kumamoto, Japan, pp 352–354

 doi:10.20944/preprints202603.1048.v1

23. State General Administration of the People's Republic of China for Quality Supervision and Inspection andQuarantine, Standardization Administration of the People's Republic of China (2011) Human dimensions of Chinese minors
24. AramisFernandez (2021) ANATOMY MODELS SCANNER. In: Cults 3D. https://cults3d.com/en/3d-model/art/anatomy-models-scanner
25. Public Health Ophthalmology Branch of Chinese Preventive Medicine Association, Wang N (2022) Chinese expert consensus on the reference interval of ocular hyperopia reserve, axial length, corneal curvature and genetic factors in school-age children (2022). Chin J Ophthalmol 58:96–102. https://doi.org/10.3760/cma.j.cn112142-20210603-00267
26. Gabriel C, Gabriel S, Corthout E (1996) The dielectric properties of biological tissues: I. Literature survey. Phys Med Biol 41:2231–2249. https://doi.org/10.1088/0031-9155/41/11/001
27. Zhou W-Y, Zhang X-Y, Lu M (2024) Electromagnetic exposure analysis of the subway passenger under the civil communication system radiation. PLOS One 19:e0300049. https://doi.org/10.1371/journal.pone.0300049
28. International Commission on Non-Ionizing Radiation Protection (ICNIRP) (2020) Guidelines for Limiting Exposure to Electromagnetic Fields (100 kHz to 300 GHz). Health Phys 118:483–524. https://doi.org/10.1097/HP.0000000000001210
29. Chiaramello, E., Bonato, M., Fiocchi, S., Tognola, G., Parazzini, M., Ravazzani, P., & Wiart, J. (2019). Radio Frequency Electromagnetic Fields Exposure Assessment in Indoor Environments: A Review. International Journal of Environmental Research and Public Health, 16(6), 955. https://doi.org/10.3390/ijerph16060955
30. Hou, W.-Q., Li, Y.-X., Luo, M.-F., Zhou, W.-Y., & Lu, M. (2026). Mobile phone MIMO antenna array miniaturization-based low SAR research in the combined EMF. PLOS One, 21(1), e0340681. https://doi.org/10.1371/journal.pone.0340681